Journal of Biomolecular NMR (2007) 37:43–51
DOI 10.1007/s10858-006-9098-6

Article

Assignment of paramagnetic ^{15}N-HSQC spectra by heteronuclear exchange spectroscopy

Michael John[a], Madeleine J. Headlam[a,b], Nicholas E. Dixon[a] & Gottfried Otting[a,*]
[a]*Research School of Chemistry, Australian National University, Canberra, ACT 0200, Australia;* [b]*Protein Discovery Centre, Queensland Institute of Medical Research, Brisbane, QLD 4029, Australia*

Received 7 July 2006; Accepted 15 September 2006

Key words: epsilon subunit, lanthanides, metal exchange, ^{15}N-HSQC assignment, N_Z-exchange spectroscopy, paramagnetic relaxation enhancement

Abstract

Paramagnetic metal ions in proteins provide a rich source of structural information, but the resonance assignments required to extract the information can be challenging. Here we demonstrate that paramagnetically shifted ^{15}N-HSQC cross-peaks can be assigned using N_Z-exchange spectroscopy under conditions in which the paramagnetic form of the protein is in dynamic equilibrium with its diamagnetic form. Even slow exchange of specifically bound metal ions may be detected within the long lifetime of ^{15}N longitudinal magnetization of large proteins at high magnetic fields. Alternatively, the exchange can be accelerated using an excess of metal ions. In the resulting exchange spectra, paramagnetic ^{15}N resonances become visible for residues that are not directly observed in a conventional ^{15}N-HSQC spectrum due to paramagnetic $^1H^N$ broadening. The experiments are illustrated by the 30 kDa lanthanide-binding ε186/θ complex of DNA polymerase III in the presence of sub-stoichiometric amounts of Dy^{3+} or a mixture of Dy^{3+} and La^{3+}.

Abbreviations: 1D – one-dimensional; CSA – chemical shift anisotrophy; ε186 – N-terminal 185 residues of the ε subunit of *E. coli* DNA polymerase III; EXSY – exchange spectroscopy; HSQC – heteronuclear single quantum correlation; INEPT – insensitive nuclei enhanced by polarization transfer.

Introduction

The interaction between the unpaired electrons of a paramagnetic metal ion and nuclear spins gives rise to a range of paramagnetic NMR effects including pseudocontact shifts, relaxation enhancements, cross-correlated relaxation and residual dipolar couplings (Bertini et al., 2002; Pintacuda et al., 2004). These effects present a rich source of structural information about biomolecules and their complexes. As a drawback, their measurement requires resonance re-assignment of the paramagnetic state. If a structural model of the molecule and the assignment of a diamagnetic reference are available, the most common approach for the assignment of paramagnetic NMR spectra is an iterative procedure that includes the following steps: (i) assignment of a small subset of resonances, (ii) fitting of the tensor of the magnetic susceptibility anisotropy, and (iii) prediction of the entire paramagnetic spectrum from the tensor and the structure (Baig et al., 2004). This procedure can be automated, yielding reliable susceptibility tensors and mostly correct assignments of ^{15}N-HSQC and HNCO spectra of paramagnetic proteins (Schmitz et al., 2006).

*To whom correspondence should be addressed. E-mail: go@rsc.anu.edu.au

In the absence of structural information, however, correlating paramagnetic with diamagnetic ^{15}N-HSQC peaks is more difficult. Particularly in the vicinity of the metal ion, peaks are often shifted from their diamagnetic position by several ppm and no longer along the 'diagonal', i.e. by the same amount in both spectral dimensions. Even if the protein structure is available, relatively small structural variations or mobility of the protein or the metal ion can result in significant deviations between measured and predicted paramagnetic shifts. Since another sequential assignment using traditional triple-resonance techniques is rather cumbersome and limited by the sensitivity of the experiments, an alternative structure-independent method for transferring diamagnetic assignments would be useful. In this paper we show that assignments of paramagnetic peaks can be established using exchange spectroscopy under conditions in which diamagnetic and paramagnetic protein states coexist and equilibrate through binding and dissociation of the metal ion.

2D exchange spectroscopy (EXSY) is an established method for the identification of spins that exchange magnetization by either cross-relaxation or chemical exchange (Jeener et al., 1979). In macromolecules, where the longitudinal magnetization present during the mixing period relaxes much more slowly than transverse magnetization, the experiment allows the detection of dynamic processes that are too slow to affect the lineshapes. To overcome the problem of overlap in the ^{1}H NMR spectra of proteins, experiments have been proposed that exploit the increased resolution of heteronuclear correlation spectra (Montelione and Wagner, 1989; Wider et al., 1991). These experiments yield HSQC-type spectra, but with additional 'exchange' peaks appearing at the opposite corners of a rectangle spanned by the conventional HSQC or 'auto' peaks. Farrow et al. (1994) have designed a variant that uses pure ^{15}N longitudinal magnetization and therefore allows the simultaneous measurement of exchange and ^{15}N longitudinal relaxation rates. This 'N_z-exchange' experiment has been employed to study folding/unfolding equilibria (Farrow et al., 1994; Zeeb and Balbach, 2005), proline *cis*/*trans* isomerizations (Bosco et al., 2002; Wang et al., 2005), and slow complex formation (Vialle-Printemps et al., 2000; Iwahara and Clore, 2006). Here we show that it is also suitable for correlating diamagnetic and paramagnetic ^{15}N-HSQC peaks in a 30 kDa complex of the lanthanide-binding N-terminal domain of the ε subunit of DNA polymerase III and the subunit θ (ε186/θ), which is loaded either partially with Dy^{3+} or with a mixture of Dy^{3+} and diamagnetic La^{3+}. The active site of ε186 is capable of binding a single lanthanide ion under the conditions of these experiments (Pintacuda et al., 2004).

Materials and methods

NMR spectroscopy

All NMR experiments were carried out at 25 °C using a Bruker AV 800 MHz NMR spectrometer equipped with a cryogenic TCI probe. The preparation of isotope labeled proteins and assembly of the ε186/θ complex have been described earlier (Hamdan et al., 2002a). Buffer conditions were 100 mM NaCl, 20 mM Tris (pH 7.2), 0.01% (w/v) NaN_3, and 0.1 mM dithiothreitol in 90% H_2O/10% D_2O. Protein concentrations were 0.9 mM for a sample with ^{2}H/^{15}N-labeled ε186 and 1.2 mM for a sample with ^{15}N-labeled θ. Lanthanides (Ln^{3+}) were added as 30 mM buffered $LnCl_3$ stock solutions. Series of N_Z-exchange spectra were recorded with the sequence as shown in Figure 1A (Farrow et al., 1994), using mixing periods (τ_m) of 0.01, 0.06, 0.12, 0.24, 0.48, 0.96, and 1.92 s. To account for fast paramagnetic $^{1}H^{N}$ relaxation, the corresponding INEPT delays (τ_H) were shortened to 1.8 ms. Each experiment was acquired in 2–3 h using a recycle delay of 3 s. For resonance assignment, both N_Z-exchange and reference (Figure 1B) spectra were recorded with $\tau_m = 0.96$ s in 16 h each using a recycle delay of 1.5 s.

Data analysis

The NMR spectra were processed using square sine-bell apodization in both dimensions and analyzed with SPARKY (Goddard and Kneller, University of San Francisco, CA, USA). Peak volumes were approximated as the product of peak intensity and linewidth of a Gaussian lineshape fitted in the $^{1}H^{N}$ dimension, assuming uniform linewidths in the ^{15}N dimension. The peak volumes of any given residue were simultaneously fit to the following equations:

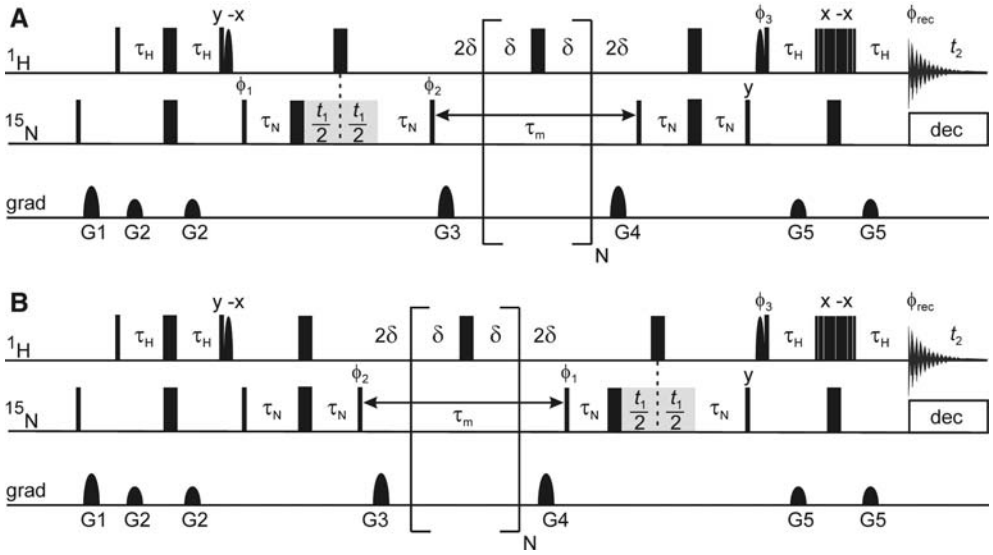

Figure 1. Pulse sequences for (A) N_z-exchange (Farrow et al., 1994) and (B) reference experiments. Both sequences differ only in the order of t_1 evolution (highlighted in gray) and mixing periods (τ_m). Narrow and wide bars indicate 90° and 180° pulses, respectively, which are applied with phase x unless indicated otherwise. The cycled phases were $\phi_1(x,-x)$, $\phi_2(2x,-2x)$, $\phi_3(4x,4y,-4x,-4y)$, and $\phi_{rec}(x,-2x,x,y,-2y,y,-x,2x,-x,-y,2y,-y)$. The water-selective 90° pulse had a 2 ms Gauss shape, and for water suppression the binomial 3-9-19 pulse train was used with a delay of 100 μs between the pulses. The delays τ_H, τ_N and δ were set to 3.6, 5.4 and 1.5 ms, respectively, and the gradient strengths were G1 = 25 G/cm, G2 = 8 G/cm, G3 = 15 G/cm, G4 = 20 G/cm, and G5 = 10 G/cm. The pulse sequences were slightly modified from the original experiment to include non-selective inversion pulses during τ_m. Although this scheme tends to saturate the water resonance, adequate water suppression was obtained on a cryogenic probe. Notably, the recovery of water equilibrium polarization is accelerated by paramagnetic relaxation enhancement.

$$
\begin{aligned}
V_{dd}(\tau_m) &= V_0(f_d^2 + f_d f_p e^{-k_{ex}\tau_m})e^{-R_1\tau_m} \\
V_{pp}(\tau_m) &= V_0(f_p^2 + f_d f_p e^{-k_{ex}\tau_m})e^{-R_1\tau_m}e^{-4\lambda\tau_H} \\
V_{dp}(\tau_m) &= V_0(f_d f_p - f_d f_p e^{-k_{ex}\tau_m})e^{-R_1\tau_m}e^{-2\lambda\tau_H} \\
V_{pd}(\tau_m) &= V_0(f_d f_p - f_d f_p e^{-k_{ex}\tau_m})e^{-R_1\tau_m}e^{-2\lambda\tau_H} \quad (1)
\end{aligned}
$$

where 'dd' and 'pp' denote the diamagnetic and paramagnetic auto peak, respectively, 'dp' and 'pd' denote the exchange peaks arising from transitions from the diamagnetic to the paramagnetic state, and vice versa, f_d and f_p ($= 1 - f_d$) are the fractional populations of diamagnetic and paramagnetic protein, R_1 is the ^{15}N longitudinal relaxation rate (assumed to be the same for diamagnetic and paramagnetic states), and k_{ex} is the exchange rate. λ accounts for enhanced relaxation of paramagnetic versus diamagnetic $^1H^N$ transverse magnetization during the INEPT (τ_H) delays (Tollinger et al., 2001) and was not fitted, but estimated from the $^1H^N$ linewidths. Full recovery of $^1H^N$ equilibrium magnetization between two scans was assumed. Fitting was performed with a routine implemented in MATLAB (MathWorks, Natick, MA, USA).

Results

Paramagnetic assignment of ε186

In a titration experiment of the ε186/θ complex with lanthanides (Ln^{3+}), the free protein and the ε186/θ/Ln^{3+} complex equilibrate slowly, so that their ^{15}N-HSQC spectra coexist in the presence of sub-stoichiometric quantities of Ln^{3+}. In complex with Dy^{3+}, the number of peaks is greatly reduced due to paramagnetic line broadening beyond detection for residues within about 15 Å distance from the paramagnetic center. Most of the remaining paramagnetic peaks were readily assigned from the diamagnetic spectrum (DeRose et al., 2003) based on paramagnetic shifts predicted from the crystal structure of ε186 (Hamdan et al., 2002b) and the susceptibility tensor of Dy^{3+} (Schmitz et al., 2006).

Yet, even 3D HNCO spectra recorded of $^{13}C/^{15}N$-labeled ε186/θ failed to confidentially assign a number of strongly paramagnetically shifted peaks, for which the $^{13}C'$, ^{15}N and $^{1}H^{N}$ shifts substantially deviated from each other and also from the predicted values (Schmitz et al., 2006). Many of these peaks could, however, be assigned with the N_Z-exchange experiment using a sample of ε186/θ with uniformly $^{2}H/^{15}N$ labeled ε186 and unlabeled θ in the presence of 0.33 equivalents of Dy^{3+}. In this sample, the $^{1}H^{N}$ NMR linewidth is minimized due to deuteration and the low concentration of free metal ions that could potentially bind to additional sites on the protein surface.

Figure 2 shows the difference spectrum of N_z-exchange and reference spectra of this sample acquired with a mixing time of $\tau_m = 0.96$ s. Subtraction of the reference from the exchange spectrum generates auto and exchange peaks of equal intensity but with opposite sign, while auto peaks with zero paramagnetic shift disappear. All paramagnetic ^{15}N-HSQC peaks (the 'pp' peaks) with $\delta(^{1}H^{N}) > 10$ ppm show the presence of 'dp' exchange peaks at the same $\delta(^{1}H^{N})$ position, so that the corresponding diamagnetic ^{15}N-HSQC peaks (the 'dd' peaks) can easily be identified. In this way, we were able to establish eight new resonance assignments of ε186 in the ε186/θ/Dy^{3+} complex (Table 1), including the resolution of two overlapping paramagnetic ^{15}N-HSQC peak pairs (N19/E153 and F79/R151). The other newly assigned residues show significant deviations between measured and predicted paramagnetic shifts as they belong either to the ε186/θ interface (F72) or a loop region (R151 and D155–K158), which may assume a different conformation in solution than in the single crystal. Deviations from the crystal structure are also evidenced by the fact that S157 and K158 are well observable in the ^{15}N-HSQC spectrum despite their short predicted $^{1}H^{N}$ distances (13.9 and 12.7 Å) to the paramagnetic center.

Residue E37 (highlighted in Figure 2) provides an example where the N_z-exchange spectrum reveals not only correlations between existing diamagnetic and paramagnetic ^{15}N-HSQC peaks, but also pd/dd pairs for a residue whose paramagnetic $^{1}H^{N}$ resonance is too broad to be observable in a conventional ^{15}N-HSQC spectrum. In the ε186/θ/Dy^{3+} complex, this enabled the indirect measurement of ^{15}N paramagnetic shifts of an additional 12 residues located within 13.6–15.7 Å from the metal

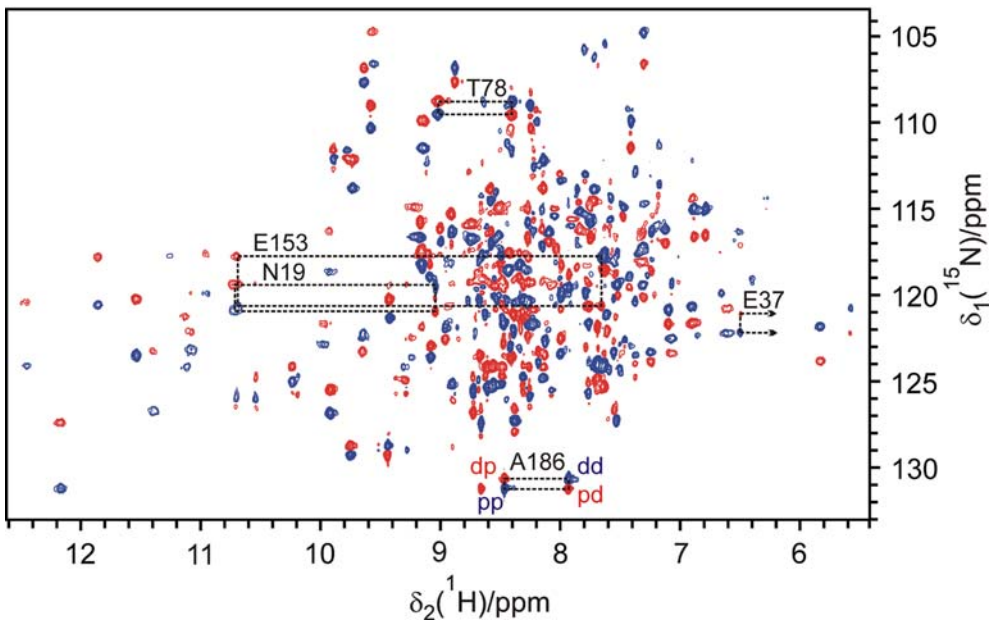

Figure 2. Difference (N_Z-exchange minus reference) spectrum of ε186/θ ($^{2}H/^{15}N$-labeled ε186) in the presence of 0.33 equivalents of Dy^{3+}. Exchange and auto peaks have opposite sign and are colored red and blue, respectively. Dashed-line rectangles highlight the four peaks dd, pd, dp, and pp of residues N19, T78, E153, and A186 of ε186. The pp peaks of N19 and E153 are overlapped, and the pp and dp peaks of E37 are unobservable due to excessive paramagnetic $^{1}H^{N}$ line broadening.

Table 1. Predicted and observed ^{15}N and $^{1}H^{N}$ paramagnetic shifts (in ppm) of newly assigned ^{15}N-HSQC peaks of ε186 in the ε186/θ/Dy^{3+} complex[a]

Residue	$r_{Dy\text{-}H}$ / Å	$\Delta\delta^{pred}$ (^{15}N)	$\Delta\delta^{obs}$ (^{15}N)	$\Delta\delta^{pred}$ ($^{1}H^{N}$)	$\Delta\delta^{obs}$ ($^{1}H^{N}$)
N19	15.4	1.4	1.5	1.39	1.66
F72	17.2	1.6	1.7	1.90	2.34
F79	17.8	1.0	1.1	1.31	1.44
R151	16.9	2.7	3.2	2.93	3.30
E153	18.4	2.9	2.9	2.86	3.05
D155	15.4	4.7	3.8	4.48	3.50
S157	13.9	2.3	2.2	2.65	2.30
K158	12.7	0.4	1.2	1.41	1.50

[a]The distances $r_{Dy\text{-}H}$ and predicted shifts are based on the crystal structure of ε186 (Hamdan et al., 2002b) and the optimized metal position and magnetic susceptibility anisotropy of Dy^{3+} (Schmitz et al., 2006). The observed values were determined as the difference in chemical shifts between the ε186/θ/Dy^{3+} and the ε186/θ/La^{3+} complex.

Table 2. Predicted and observed ^{15}N paramagnetic shifts (in ppm) of ε186 residues in the ε186/θ/Dy^{3+} complex for which shifts could only be derived from dd/pd pairs[a]

Residue	$r_{Dy\text{-}H}$ / Å	$\Delta\delta^{pred}$ (^{15}N)	$\Delta\delta^{obs}$ (^{15}N)
M18	13.6	4.6	4.5
K29	14.0	5.5	5.5
E37	15.4	−0.8	−1.0
H49	14.1	−5.2	−5.6
D59	14.3	5.6	5.9
A69	13.9	3.7	4.9
A101	13.7	−3.8	−3.9
G105	13.6	−1.9	−1.8
A132	15.1	−0.5	−0.8
A150	15.0	3.8	4.4
N156	13.9	5.0	3.7
L176	15.7	3.8	3.7

[a]See footnote of Table 1.

ion (Table 2). The measured values are in agreement with the predicted shifts, except for residues in the above mentioned loop (A150, N156) and at the ε186/θ interface (A69).

Paramagnetic assignment of θ

Since the θ subunit consists of only 76 residues, there is much less resonance overlap in ^{15}N-HSQC spectra of a sample of the ε186/θ complex in which θ is ^{15}N-labeled than for ^{15}N-labeled ε186. Further, paramagnetic line broadening is less pronounced as most of the backbone of θ is separated from the paramagnetic center by more than 15 Å (Pintacuda et al., 2006; Keniry et al., 2006). In the absence of ^{2}H-labeling, however, additional $^{1}H^{N}$ line broadening arises from unresolved $^{1}H-^{1}H$ residual dipolar couplings due to paramagnetic alignment of the protein. We prepared the sample with ^{15}N-labeled θ with 0.5 equivalents each of Dy^{3+} and La^{3+}. The ^{15}N-HSQC spectrum shows the expected 1:1 ratio of diamagnetic and paramagnetic signal sets with no evidence for the presence of the apo-protein.

Figure 3A shows the N_Z-exchange spectrum of this sample recorded with $\tau_m = 0.96$ s. From this spectrum, 51 out of 54 ^{15}N-HSQC peaks observed for the ε186/θ/Dy^{3+} complex were readily correlated with the peaks of the ε186/θ/La^{3+} complex without making use of the protein structure (Keniry et al., 2006) or any assumptions about the metal position or the magnetic susceptibility tensor. Although the 70 diamagnetic ^{15}N-HSQC peaks of ε186/θ/La^{3+} with known assignments (Keniry et al., 2006) are present in the exchange spectrum, a small number of them (mainly belonging to the N-terminus) are already broadened in the diamagnetic protein and show no corresponding exchange peaks. The mixture of Dy^{3+} and La^{3+} allows to directly read off paramagnetic shifts from the spectrum without the need for corrections due to metal binding, as required in a sample where the paramagnetic complex is in equilibrium with the apo-protein. The 51 measured shifts are in good agreement with the reported values (Keniry et al., 2006).

At a ε186/θ:La^{3+}:Dy^{3+} ratio of 1:1:1, the spectral quality is much reduced as many resonances become very broad or invisible (Figure 3B), presumably due to exchange broadening (see below) and transient binding of excess

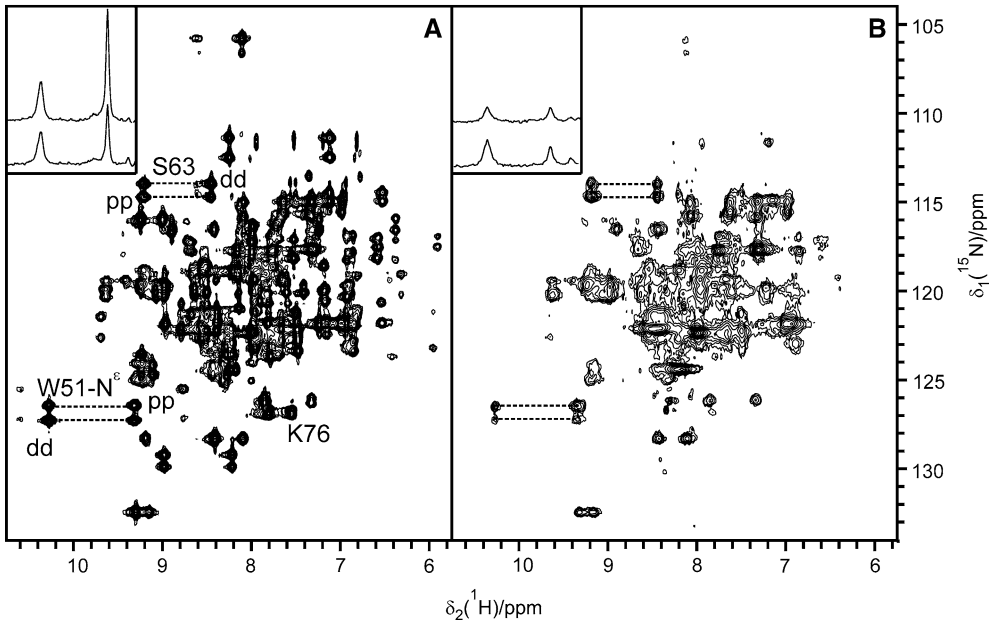

Figure 3. N_Z-exchange spectrum of ε186/θ (^{15}N-labeled θ) in the presence of 1:1 mixtures of Dy^{3+} and La^{3+}. (A) Spectrum with 1:0.5:0.5 ratio of ε186/θ:Dy^{3+}:La^{3+}. (B) Spectrum with 1:1:1 ratio of ε186/θ:Dy^{3+}:La^{3+}. Dashed-line rectangles highlight the four peaks dd, pd, dp, and pp of S63 and the sidechain N^{ε} of W51 of θ. The insert shows 1D traces through the dp/dd peaks (top) and pp/pd peaks (bottom) of S63. The C-terminal residue K76, highlighted in (A), has disappeared in (B).

Dy^{3+} at the protein surface. In particular, the intense signals of the C-terminal residue, K76, have completely disappeared, and a similar behavior was found for A186 of ε186 in the presence of excess Dy^{3+}. Both residues are mobile and remote (>25 Å) from the paramagnetic center, but their carboxyl groups present potential lanthanide binding sites. In a titration experiment using only La^{3+}, the chemical shift changes observed for these and other residues near negatively charged surface patches indeed indicated several sites with weak lanthanide binding affinities (K_D > 1 mM). In contrast, the peaks belonging to residues S63 and the sidechain N^{ε} of residue W51, both of which are buried in the hydrophobic core of θ, remain relatively narrow and well resolved. Their pp peaks have gained in strength relative to the dd peaks (see inserts of Figure 3), indicating that binding of Dy^{3+} in the active site of ε186 is slightly preferred over La^{3+}.

Metal exchange rates

The rates of metal exchange can be measured by monitoring auto and exchange peaks in a series of N_Z-exchange spectra with different mixing times (τ_m). Figure 4A shows the dd, pp, and pd peak volumes of the C-terminal residue of ε186 , A186, in the sample with 0.33 equivalents of Dy^{3+} as a function of τ_m. Since for this residue the linewidths of diamagnetic and paramagnetic $^1H^N$ resonances are indistinguishable ($\lambda = 0\ s^{-1}$), the 2:1 ratio of dd and pp peak volumes at zero mixing time reflects the populations $f_d = 0.67$ and $f_p = 0.33$ of the diamagnetic and paramagnetic protein states. Fitting of all four peaks to Equation (1) yields $R_1 = 0.84\ s^{-1}$ and $k_{ex} = 0.89\ s^{-1}$ for the rates of ^{15}N longitudinal relaxation and metal exchange, respectively. Figure 4B shows the corresponding fit for the α-helical residue T78, where paramagnetic $^1H^N$ broadening is significant ($\lambda = 30\ s^{-1}$), and $R_1 = 0.53\ s^{-1}$ is mostly governed by molecular tumbling.

Figure 4C shows the evolution of auto and exchange peaks for residue S63 of θ (^{15}N-labeled) in the presence of 0.5 equivalents each of Dy^{3+} and La^{3+}. Whereas $R_1 = 0.58$ is comparable to that of rigid residues in the deuterated ε186/θ complex in the presence of sub-stoichiometric amounts of Dy^{3+}, k_{ex} is tenfold enhanced,

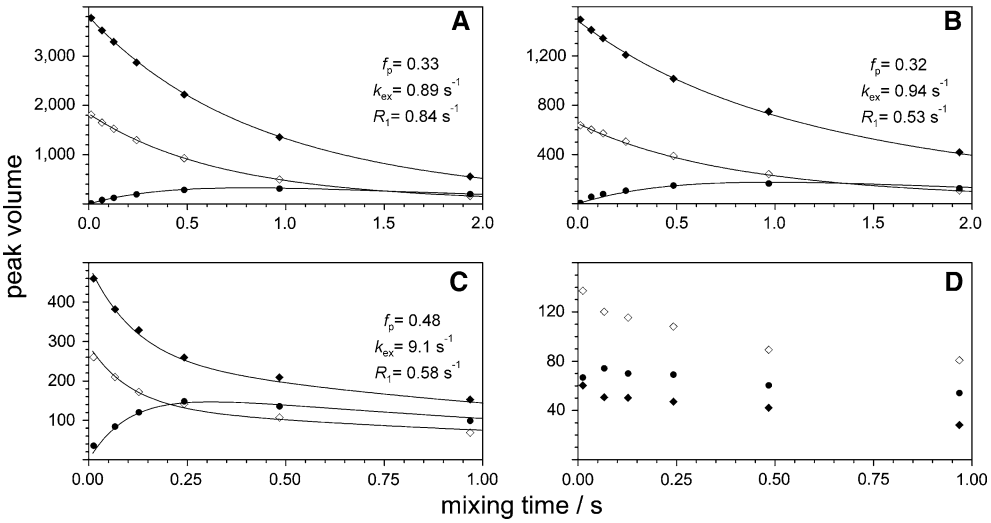

Figure 4. Volumes of auto and exchange peaks versus mixing time for selected residues. (A) A186 of ε186 in the presence of 0.33 equivalents of Dy^{3+}. (B) Same as (A), but for T78 of ε186 . (C) S63 of θ at a 1:0.5:0.5 ratio of ε186/θ:Dy^{3+}:La^{3+}. (D) S63 of θ at a 1:1:1 ratio of ε186/θ:Dy^{3+}:La^{3+}. Note the different horizontal scales in (A) and (B) versus (C) and (D). Filled and open diamonds represent dd and pp auto peaks, respectively, whereas filled circles represent the pd exchange peak. The best fit is shown with solid lines, and fit parameters are given.

resulting in maximum exchange peaks at much shorter mixing times. At $\tau_m = 0.48$ s, the equilibration between bound Dy^{3+} and La^{3+} is 99% complete, and the subsequent decay of auto and exchange peaks becomes monoexponential with R_1 as rate constant. Since $f_d \approx f_p$, the difference in their peak volumes can be attributed to the different $^1H^N$ relaxation properties during the INEPT delays of the pulse sequence.

Figure 4D shows the same plot as Figure 4C, but in the presence of 1 equivalent each of Dy^{3+} and La^{3+}. Although both diamagnetic and paramagnetic $^1H^N$ resonances of S63 are much broader (see Figure 3A, B), the enhancement of paramagnetic versus diamagnetic $^1H^N$ relaxation remains essentially unchanged ($\lambda = 70$ s^{-1}). The pp peaks are now stronger than the dd peaks, reflecting the favored binding of Dy^{3+} over La^{3+} to ε186/θ. Due to the scarcity of data points at short mixing times, fitting did not yield stable results, but we could estimate $k_{ex} > 90$ s^{-1} from exchange peak maxima at $\tau_m < 0.06$ s, whereas there is no evidence for enhanced R_1. At these high exchange rates, exchange broadening (which equally affects $^1H^N$ and ^{15}N spins) is substantial, and significant equilibration occurs during the refocused INEPT transfer at zero mixing time.

Discussion

Exchange mechanism

In agreement with earlier studies on a related enzyme (Frey et al., 1996), a recent determination of the binding affinity of Dy^{3+} to ε186/θ yielded a dissociation constant of $K_D \approx 7$ μM (Park, 2006). Consequentially, at about 1 mM of ε186/θ the concentration of free Dy^{3+} ions rises from 3.5 μM at a ε186/θ:Dy^{3+} ratio of 1:0.33 to about 20-fold at a 1:1 ratio and reaches several hundred μM at a 1:2 ratio. As the concentration of free ions increases, metal binding becomes much faster than dissociation, and as a result, the equilibrium between apo-ε186/θ and ε186/θ/Dy^{3+} is shifted towards the metal-bound form leaving very little apoprotein. As La^{3+} binds slightly weaker to ε186/θ, the concentration of free La^{3+} is slightly higher than that of Dy^{3+}.

If the exchange between diamagnetic ε186/θ/La^{3+} and paramagnetic ε186/θ/Dy^{3+} and vice versa proceeded via the apo-form of the protein (i.e. a dissociative mechanism), the overall exchange rate would be limited by the slow dissociation of Ln^{3+} and not depend on the concentration of free lanthanides. In contrast, for an associative or concerted process the rates would be

expected to scale linearly with the free lanthanide concentration. As our data clearly show increased exchange rates in the presence of excess Ln^{3+} ions, metal exchange under these conditions seems to be mostly associative or concerted. Similar observations have been made for the replacement of Ca^{2+} by Ce^{3+} in calbindin (Barbieri et al., 2002). The possibility to manipulate metal exchange rates by control of the metal concentration would make a wide range of metalloproteins amenable to exchange spectroscopy, in particular those that bind metals more tightly than ε186/θ.

Resonance assignment

Exchange between diamagnetic and paramagnetic molecules has been employed for resonance assignment before. Homonuclear 2D EXSY experiments have been used to assign NMR spectra of a Co^{2+} complex of the peptide antibiotic bacitracin (Epperson and Ming, 2000) and to monitor metal exchange in chelate complexes (Chapon et al., 2002; Yang et al., 2002). In addition, Donaire et al. (2002) have used ^1H saturation transfer by metal exchange for resonance assignment in the small blue copper(II) proteins pseudoazurin and rusticyanin. In these systems, however, very short mixing times and elevated temperatures had to be used in order to observe exchange peaks in the presence of significant paramagnetic ^1H relaxation. The heteronuclear experiment used here offers several advantages:

(i) Heteronuclear magnetization is much less sensitive with respect to paramagnetism. This is easily understood by considering the relaxation rates predicted for an isolated $^1H^N$–^{15}N spin pair in the ε186/θ/Dy^{3+} complex (Table 3). Under conditions where $^1H^N$ transverse relaxation starts to prevent ^{15}N-HSQC detection of that spin pair, the corresponding ^{15}N spin is barely affected by paramagnetic enhancement of either longitudinal (R_1) or transverse (R_2) relaxation. In macromolecules, the paramagnetic enhancement of R_1 is independent of the nuclear gyromagnetic ratio and therefore equally small for the $^1H^N$ spin. In smaller molecules, where molecular tumbling becomes faster than the heteronuclear Larmor frequency, this degeneracy is lifted in favor of the heteronuclear spin.

(ii) Heteronuclear longitudinal magnetization generally relaxes more slowly than ^1H longitudinal magnetization. Due to dipolar interactions with other protons and exchange with the bulk water magnetization (Pervushin et al., 2002; Hiller et al., 2005), longitudinal relaxation of protons is usually much faster ($>1\ s^{-1}$) than predicted for an isolated $^1H^N$–^{15}N spin pair (Table 3). At 800 MHz, this makes N_Z magnetization the most slowly relaxing magnetization available in ^{15}N-labeled proteins with a molecular weight >15 kDa. The long lifetime of N_Z magnetization in large proteins has earlier been used for the measurement of diffusion coefficients (Ferrage et al., 2003). Here we could show that it also allows the observation of remarkably slow exchange processes with rate constants below $1\ s^{-1}$. Rates of even slower processes can be measured by NMR in real time using stopped-flow techniques (Barbieri et al., 2002).

(iii) Heteronuclear spins of paramagnetic proteins can be addressed indirectly from exchange peaks detected on the diamagnetic ^1H NMR resonance. As these exchange peaks are affected by fast paramagnetic ^1H transverse relaxation only during the period required to create N_Z magnetization (INEPT), we could observe them for ^{15}N spins so close to the paramagnetic center that the corresponding $^1H^N$ NMR signals are broadened by up to 140 Hz. This makes heteronuclear exchange spectroscopy an attractive alternative to heteronuclear direct detection (Sadek and Brownlee, 1995; Babini et al., 2004).

(iv) Heteronuclear correlation spectra present a more suitable format for the assignment of paramagnetic resonances than homonuclear spectra due to the generally higher

Table 3. Contributions of CSA, dipole–dipole (DD), and Curie mechanisms to longitudinal (R_1) and transverse (R_2) relaxation rates (in s^{-1}) in a ^{15}N–$^1H^N$ spin pair[a]

Mechanism	R_1 (^{15}N)	R_1 ($^1H^N$)	R_2 (^{15}N)	R_2 ($^1H^N$)
CSA	0.22	0.0006	11	3
DD	0.34	0.01	17	17
Curie	0.04	0.04	2	200

[a]Calculated for a distance of 15 Å from a Dy^{3+} ion in a 30 kDa protein ($\tau_C = 17$ ns) at a magnetic field of 18.8 T (800 MHz).

heteronuclear chemical shift dispersion. In the case of the 76-residue protein θ, nearly complete ^{15}N-HSQC assignment of the paramagnetic state could be obtained from a single experiment.

In conclusion, we anticipate N_Z-exchange spectroscopy to become a routine tool in the resonance assignment of paramagnetic proteins.

Acknowledgments

M.J. thanks the Humboldt Foundation for a Feodor Lynen Fellowship. Financial support from the Australian Research Council for a Federation Fellowship for G.O., project grants and the 800 MHz NMR spectrometer at the Australian National University is gratefully acknowledged.

References

Babini, E., Bertini, I., Capozzi, F., Felli, I.C., Lelli, M. and Luchinat, C. (2004) *J. Am. Chem. Soc.*, **126**, 10496–10497.

Baig, I., Bertini, I., Del Bianco, C., Gupta, Y.K., Lee, Y.-M., Luchinat, C. and Quattrone, A. (2004) *Biochemistry*, **43**, 5562–5573.

Barbieri, R., Hore, P.J., Luchinat, C. and Pierattelli, R. (2002) *J. Biomol. NMR*, **23**, 303–309.

Bertini, I., Luchinat, C. and Parigi, G. (2002) *Prog. NMR Spectrosc.*, **40**, 249–273.

Bosco, D.A., Eisenmesser, E.Z., Pochapsky, S., Sundquist, W.I. and Kern, D. (2002) *Proc. Natl. Acad. Sci. USA*, **99**, 5247–5252.

Chapon, D., Delangle, P. and Lebrun, C. (2002) *J. Chem. Soc. Dalton Trans.*, 68–74.

De Rose, E.F., Li, D., Darden, T., Harvey, S., Gabel, A., Perrino, F.W., Schaaper, R.M. and London, R.E. (2003) *Biochemistry*, **42**, 3635–3644.

Donaire, A., Jiménez, B., Fernández, C.O., Pieratelli, R., Niizeki, T., Moratal, J.-M., Hall, J.F., Kohzuma, T., Hasnain, S.S. and Vila, A.J. (2002) *J. Am. Chem. Soc.*, **124**, 13698–13708.

Epperson, J.D. and Ming, L.-J. (2000) *Biochemistry*, **39**, 4037–4045.

Farrow, N.A., Zhang, O., Forman-Kay, J.D. and Kay, L.E. (1994) *J. Biomol. NMR*, **4**, 727–734.

Ferrage, F., Zoonens, M., Warschawski, D.E., Popot, J.-L. and Bodenhausen, G. (2003) *J. Am. Chem. Soc.*, **125**, 2541–2545.

Frey, M.W., Frey, S.T., Horrocks, W.D. Jr., Kaboord, B.F. and Benkovic, S.J. (1996) *Chem. Biol.*, **3**, 393–403.

Hamdan, S., Bulloch, E.M., Thompson, P.R., Beck, J.L., Yang, J.Y., Crowther, J.A., Lilley, P.E., Carr, P.D., Ollis, D.L., Brown, S.E. and Dixon, N.E. (2002a) *Biochemistry*, **41**, 5266–5275.

Hamdan, S., Carr, P.D., Brown, S.E., Ollis, D.L. and Dixon, N.E. (2002b) *Structure*, **10**, 535–546.

Hiller, S., Wider, G., Etezady-Esfarjani, T., Horst, R. and Wüthrich, K. (2005) *J. Biomol. NMR*, **32**, 61–70.

Iwahara, J. and Clore, G.M. (2006) *J. Am. Chem. Soc.*, **128**, 404–405.

Jeeener, J., Meier, B.H., Bachmann, P. and Ernst, R.R. (1979) *J. Chem. Phys.*, **71**, 4546–4553.

Keniry, M.A., Park, A.Y., Owen, E.A., Hamdan, S.M., Pintacuda, G., Otting, G. and Dixon, N.E. (2006) *J. Bacteriol.*, **188**, 4464–4473.

Montelione, G.T. and Wagner, G. (1989) *J. Am. Chem. Soc.*, **111**, 3096–3098.

Park, A.Y. (2006) PhD thesis, Australian National University.

Pervushin, K., Vögeli, B. and Eletsky, A. (2002) *J. Am. Chem. Soc.*, **124**, 12898–12902.

Pintacuda, G., Keniry, M.A., Huber, T., Park, A.Y., Dixon, N.E. and Otting, G. (2004) *J. Am. Chem. Soc.*, **126**, 2963–2970.

Pintacuda, G., Park, A.Y., Keniry, M.A., Dixon, N.E. and Otting, G. (2006) *J. Am. Chem. Soc.,* **128**, 3696–3702.

Sadek, M. and Brownlee, R.T.C. (1995) *J. Magn. Reson. Ser. B*, **109**, 70–75.

Schmitz, C., John, M., Park, A.Y., Pintacuda, G., Dixon, N.E., Otting, G. and Huber, T. (2006) *J. Biomol. NMR*, **35**, 79–87.

Tollinger, M., Skrynnikov, N.R., Mulder, F.A.A., Forman-Kay, J.D. and Kay, L.E. (2001) *J. Am. Chem. Soc.*, **123**, 11341–11352.

Vialle-Printemps, C., van Heijenoort, C. and Guittet, E. (2000) *J. Magn. Reson.*, **142**, 276–279.

Wang, X., Tong, S. and Wang, Y. (2005) *Biochem. Biophys. Res. Commun.*, **329**, 495–501.

Wider, G., Neri, D. and Wüthrich, K. (1991) *J. Biomol. NMR*, **1**, 93–98.

Yang, L., Crans, D.C., Miller, S.M., la Cour, A., Anderson, O.P., Kaszynski, P.M., Godzala, M.E. III, Austin, L.D. and Willsky, G.R. (2002) *Inorg. Chem.*, 41, 4859–4871.

Zeeb, M. and Balbach, J. (2005) *Protein Pept. Lett.*, **12**, 139–146.